NUMERICAL INVESTIGATION OF FLOW OVER MULTI-ELEMENT AIRFOILS WITH LIFT-ENHANCING TABS

Zhenhui Zhang, Dong Li
National Key Laboratory of Science and Technology on Aerodynamic Design and Research, Northwestern Polytechnical University, Xi'an 710072, China
zhenhui224@mail.nwpu.edu.cn; ldgh@nwpu.edu.cn

Keywords: *high-lift systems; multi-element airfoils; lift-enhancing tabs; SST k-ω turbulence model; multi-block structured grids*

Abstract

The flow over multi-element airfoils with flat-plate lift-enhancing tabs placed near the trailing edge of main element or/and flap was numerically investigated for different flap riggings. The 2D unsteady Reynolds-Averaged Navier-Stokes (RANS) equations together with the two-equation SST k-ω turbulence model were applied to this numerical simulation utilizing the multi-block structured grids of C-H type. The effects of local grid near the lift-enhancing tabs on computational results and also various tabs were studied for McDonnell Douglas Aerospace three-element airfoils consisting of a slat and single-slotted flap. Numerical results showed that the impact of lift-enhancing tabs on the performance of multi-element airfoils depended on the location and height of tabs and multi-element configurations. The cove tab could reduce the amount of separated flow on the flap being in non-optimum position, whereas the flap tab could substantially increase the lift of multi-element airfoils for different configurations, and the combination tab was approximately a linear combination of the changes caused by the individual tabs.

1 General Introduction

The High-lift capability of an aircraft, affecting take-off and landing performance and low-speed maneuverability, plays an important role in the design of military and commercial aircraft. Improved high-lift performance can lead to increased range and payload as well as decreased landing speed and field length requirements. The take-off configuration designed for a high lift-to-drag ratio (L/D) at moderate lift coefficient is different from the landing configuration designed for high maximum lift coefficient. Typical high-lift system for transport aircraft often consisting of a basic wing with a leading-edge slat and trailing-edge flap elements is highly efficient aerodynamically, but at the expense of complex structure and expensive design and maintenance costs. Current design effects have focused on mechanically simpler high-lift systems that incorporate advanced technology to meet design requirements.

Valarezo [1] et al. carried out an experimental investigation of drooped spoilers and trailing-edge wedges on an advanced three-element airfoil. Deflecting the spoiler 5 and 10 degree downward could lead to a considerable increase in lift at lower angles of attack and a decrease in stall angle and maximum lift coefficient. The wedges with constant length of 3% chord and different heights determined by wedge angle produced a lift increment that was largest at 0° angle of attack and diminished as the angle of attack was increased. Most of the lift increment was attributed to the augmented loading of the main element other than the flap.

The European AWIATOR program had demonstrated the use of vortex generators [2] on an aircraft of Airbus type configuration in wind tunnel test conditions. On the basis of the measurements, Brunet [3] et al carried out Navier-Stokes steady computations on a wing cross section (44% of the wing span) to simulate and analyze the VGs effect on the separated

flow on the flap of the high-lift system in landing conditions. The comparisons between experiments and RANS computations had shown a very good agreement and a great efficiency of the VGs flow control system.

Lift-enhancing tabs, similar to Gurney flap [4] , have received considerable attention over the last few years and appear to be a promising means of improving high-lift performance. The Gurney flap originally used on the airfoils of race cars to increase the downforce for the lateral traction is a flat plate device which is mounted perpendicular to the trailing edge of the furthest downstream wing element. What is slightly different from Gurney flap is that lift-enhancing tabs retracted within the cruise-wing contour can be attached to the trailing edge of any or all elements of multi-element airfoil. Much work has been performed by a number of researchers [4] [5] [6] [7] to the investigation of lift-enhancing tabs on single-element and two-element airfoils. Storms [5] et al. conducted an experimental investigation of lift-enhancing tabs mounted at the trailing edge of the main element and flap of two-element airfoil NACA63(2)-215B with a 30% chord slotted flap in the NASA Ames Research Center 7- by 10-Foot Wind Tunnel. The computational investigation by Carrannanto [7] exhibited similar trends to those observed in the experimental results. It appears that few studies are concerned with the application of lift-enhancing tabs to three-element airfoils.

In this study, lift enhancing tabs were numerically investigated on McDonnell Douglas Aerospace (MDA) three-element airfoil [8] for different flap riggings. A sketch of the airfoil geometry and associated parameters are shown in Fig.1. The lift-enhancing tabs located near the trailing edge of main element and flap will be referred to as cove tab and flap tab respectively, and combination of the two as combination tab. For convenience, the distance of 1.00% of reference chord from the trailing edge is denoted as D1.00, and the height of 0.50% of reference chord as H0.50, and so on. All computations in this paper were performed at Reynolds number of 9.0×10^6 and Mach number of 0.2.

2 Numerical Investigation

2.1 Computational Method

The 2D unsteady Reynolds-Averaged Navier-Stokes (RANS) equations were applied to this numerical simulation using the finite volume method. The discretized schemes of the convective fluxes, diffusive fluxes and unsteady terms were all of second-order accuracy and the resulting equations were solved with implicit pseudo-time stepping scheme. In this study, fully turbulent computations were performed using the two-equation SST k-ω turbulence model. In addition to no-slip wall boundary condition applied at the airfoil surface, pressure farfield boundary condition were used.

The grids used in this study were the multi-block structured grids of C-H type, with normal grid spacings of 10^{-5} reference chords at the surface. As for computational domain, the upstream and downstream distances from the airfoil were 20 reference chords, and the others were 15 reference chords.

2.2 Numerical Validation

The baseline configuration of MDA three-element airfoil 30P30N, as shown in Fig.1, is used here as a validation case of numerical methods. Many efforts of multi-element airfoils computation have been made to various MDA three-element configurations [9] [10] , tested over the course of many years (primarily the 1990s) in the NASA Langley LTPT. For the 30P30N configuration with both slat and flap deflected 30°, the slat overlap and gap defined in Fig.1 are -2.50 and 2.95 percent of undeflected airfoil chord, and the flap overlap and gap are 0.25 and 0.89 percent respectively. A closed-up of the computational grid is shown in Fig.2.

A comparison of computed and experimental (Ref. [11]) lift coefficient versus angle of attack is shown in Fig.3. Excellent agreement with experiment is obtained for the lift coefficient at lower angles of attack, and the discrepancy in maximum lift coefficient between computation and experiment is less than 2.7%. The computed angle of attack at

which maximum lift occurs is about 23°, which is slightly larger than that of experiment.

Fig.4 plots the pressure coefficient on the surface of the elements at 16 angles of attack comparing computational results against experimental results from Ref. [10] . As can be seen from the figure, computed pressure distribution is in very good agreement with measurements.

It's worth mentioning that the computed results showed traces of small flow separation on the upper surface of the flap at angles of attack below 12°, and off-body separation in the wake of the main element at angles of attack above 20°, and fully attachment over the flap at all other angles of attack.

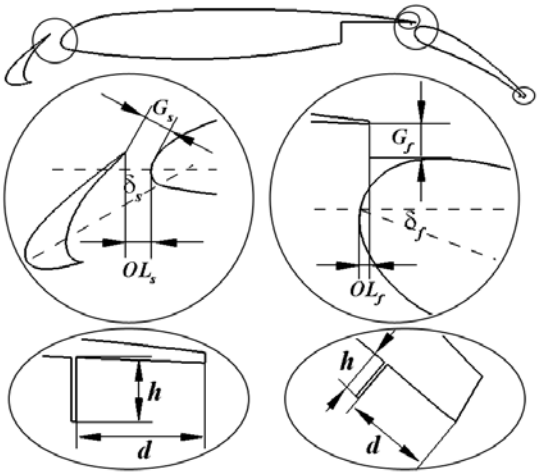

Fig.1 Geometry for three-element airfoil and associated defining parameters

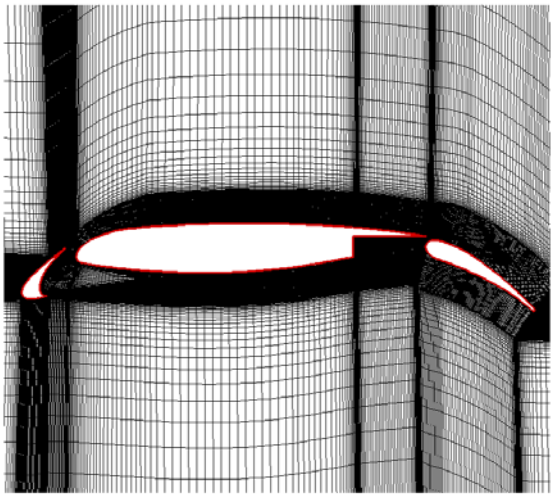

Fig.2 Multi-block structured grids of C-H type for 30P30N

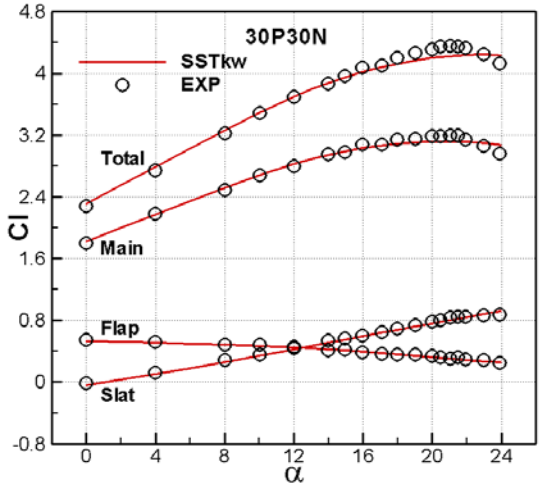

Fig.3 Comparison of Lift coefficient for 30P30N between computation and experiment

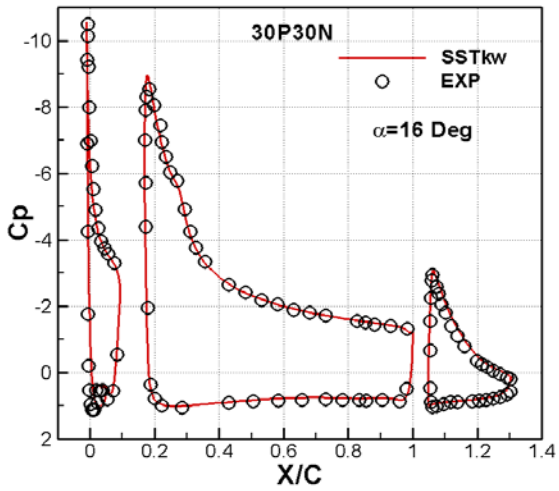

Fig.4 Comparison of computational and experimental pressure distribution for 30P30N (α=16°)

2.3 Grid Strategy

The size of lift-enhancing tabs is generally on the order of 1% of reference chord, therefore the grids that model lift-enhancing tabs would be blanked out from the baseline computational domain to simply the process of grid generation [7] . In order to illustrate this grid strategy, two kinds of grids, Grid1 and Grid2 as shown in Fig.5, were compared on the tab configurations of 30P30N (denoted as P0). Note that Grid2 with tab surface normal grid spacings of 10^{-5} chords was generated from performing grid refinement near tabs on Grid1 with tab surface normal grid spacings of the width of the tabs, 4×10^{-4} chords.

Comparisons of the computed results, including lift coefficient, drag coefficient and pitching moment coefficient, on the two kinds of grids are shown in Fig.6. Excellent agreement between the results based on these two kinds of grids is obtained for all angles of attack. In other words, the resolution of Grid1 could meet computational accuracy requirements compared to that of Grid2. Therefore, all subsequent computations, including cove tab configurations, flap tab configurations and combination tab configurations, were performed on Grid1, which could lead to considerably decreased overall grid dimensions compared to Grid2.

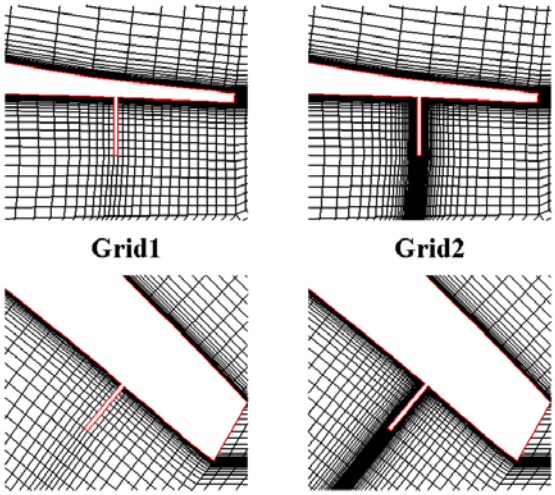

Fig.5 Two kinds of grid without and with refinement near the tabs

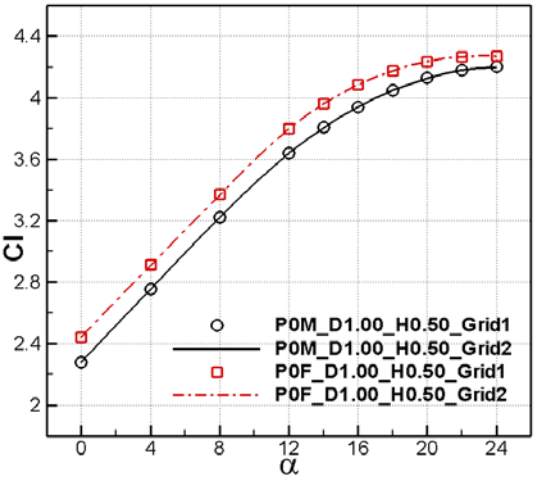

(a) Lift coefficient

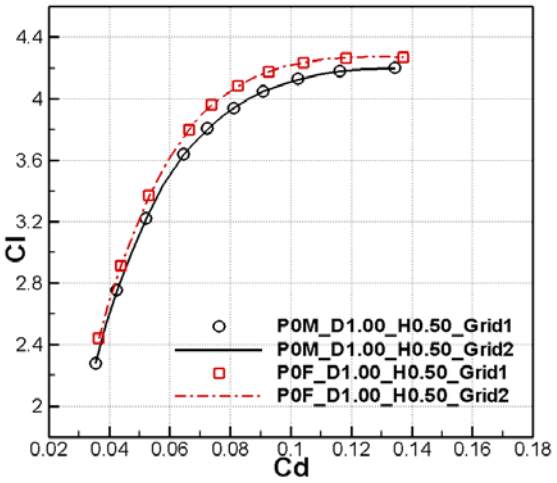

(b) Drag coefficient

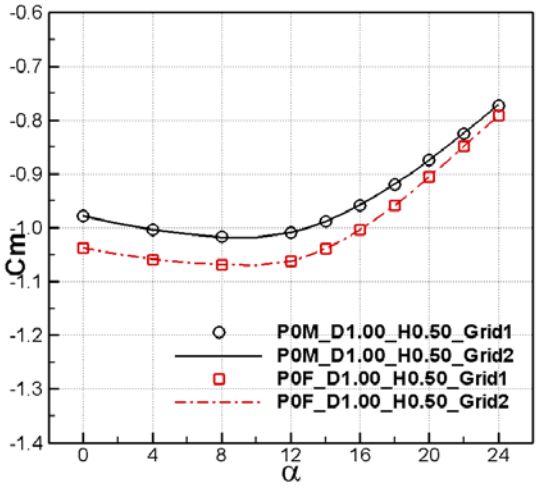

(c) Pitching moment coefficient

Fig.6 Effect of local tab grids on computational results

3 Results and Discussions

When mounted in the cove region of main element, the lift-enhancing tabs modifies the effective gap between main element trailing edge and flap. In this paper, therefore attention is being focused on the influence of lift-enhancing tabs on Douglas three-element airfoil configurations with different flap setting parameters.

3.1 Lift-enhancing tabs on configuration with moderate flap gap

Fig.7 illustrates the effect of lift-enhancing tabs on the lift, drag, and pitching moment

coefficients of the above mentioned 30P30N three-element airfoil (denoted as P0).

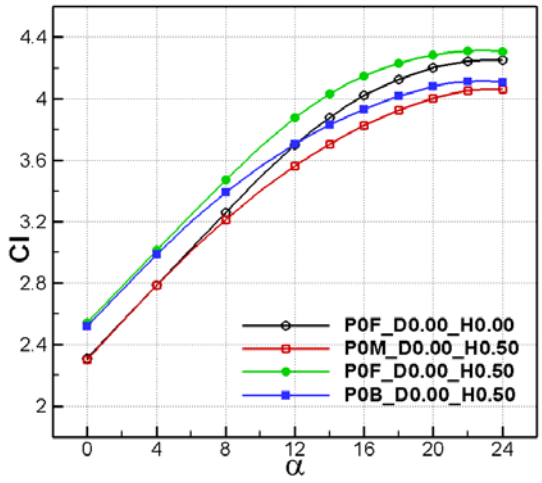

(a) Lift coefficient

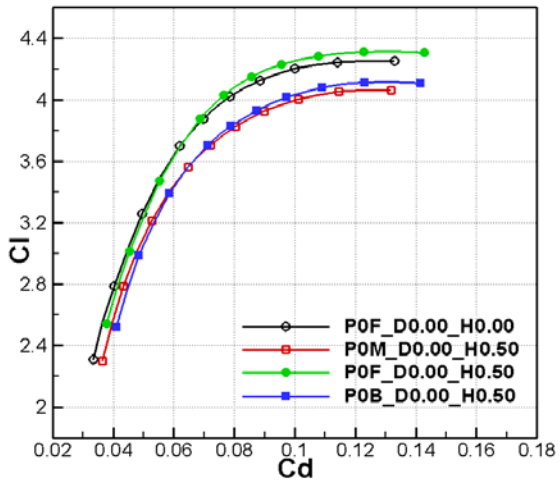

(b) Drag coefficient

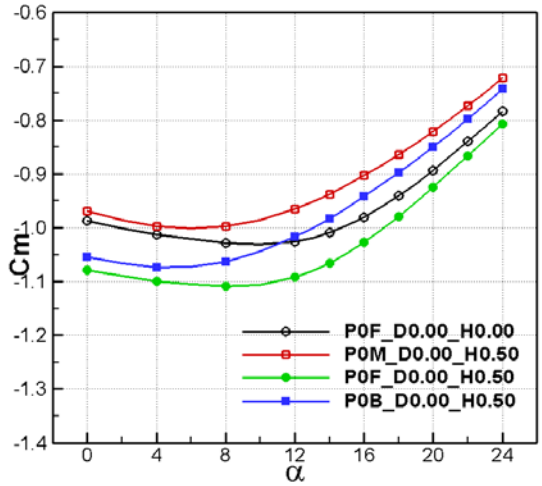

(c) Pitching moment coefficient

Fig.7 Effect of lift-enhancing tabs on the lift and moment coefficients of P0 baseline configuration

The addition of a 0.50%*c* cove tab located at the main element trailing edge does not affect the lift coefficient at low angles of attack, but the slope of the lift coefficient curve is significantly reduced as angle of attack increases, causing a reduction of 0.19 in maximum lift coefficient. Compared with the baseline configuration, the drag coefficient at a constant lift coefficient is increased at all lift coefficients and the pitching moment coefficient produces a shift in the positive direction.

When a 0.50%*c* flap tab is added to the baseline configuration, an upward shift of the lift coefficient curve is observed. The lift coefficient increment at an angle of attack of 8°, typical approach angle of attack, is 0.21, and the maximum lift coefficient increases 0.06 with the tendency of decreased stall angle. Compared with the baseline configuration, the drag coefficient remains almost unchanged and the pitching moment coefficient is shifted in the negative direction.

As shown in Fig.7, the impact on the force and moment coefficients of adding a cove tab and a flap tab combination to the baseline configuration appears to be a liner combination of the changes caused by the cove tab and the flap tab individually.

The results for flap tab configurations of several heights (0.50%*c*, 1.00%*c* and 2.00%*c*) not reported here demonstrated that as the flap tab height increased the slope of lift increment curve versus flap tab height decreased, accompanied by increased drag coefficient and pitching moment coefficient. At angle of attack of 8°, the lift increment of 0.50%*c* flap tab configuration reached 0.21 (See Fig.7), whereas the cases of 1.00%*c* and 2.00%*c* were only 0.30 and 0.38 respectively.

On the contrary, if the distance of flap tab with constant height from the flap trailing edge increased, the reduced lift coefficient was accompanied by decreased drag coefficient and pitching moment coefficient. When the 0.50%*c* flap tab was mounted 1.00%*c* upstream of flap trailing edge, lift coefficient at angle of attack of 8° reduced 0.10, compared with that at the flap trailing edge.

Based on above conclusions, the flap tab in later discussion will be placed at the flap trailing

edge, with constant height of 0.50% of reference chord. Similarly, the cove tab will be also mounted at the main element trailing edge.

3.2 Lift-enhancing tabs on configuration with high flap gap

When the flap gap of the baseline configuration was increased from 0.89%*c* to 2.89%*c*, leaving the flap deflection and overlap unchanged, the flow over a large percentage of the flap upper surface became separated. This case is clearly a non-optimum baseline configuration, as can be seen by comparing Fig.8(a) with Fig.7(a). In this case, the computed results show that a hysteresis loop [12] [13] at angles of angle between 20° and 22° occurs on the aerodynamic coefficients of the baseline configuration. The hysteresis loop was found to be counter-clockwise in lift and drag coefficients, but clockwise in pitching moment coefficient. The lift coefficient at angle of attack of 21° was found to be 4.04 along the increasing angle branch of the hysteresis loop, but 4.31 along the decreasing angle branch.

As shown in Fig.8, the effect of lift-enhancing tabs on the aerodynamic forces and moment is somewhat different than it was at smaller flap gap setting. Adding a 0.50%*c* cove tab to the baseline configuration has a significant impact on the lift coefficient curve, improving its linear property and shifting it upward to a large extent. At 8° angle of attack, the lift coefficient is increased 0.48 compared to baseline configuration. It's interesting that the drag coefficient at angles of attack prior to the hysteresis loop of the baseline configuration is reduced significantly due to the cove tab. The effect on the pitching moment of adding the cove tab is a large shift in the negative direction, corresponding with increased pitching moment coefficient.

The surface pressure distribution for the baseline and cove tab configurations are compared in Fig.9(a) at 8° angle of attack. Separation on the flap upper surface of the baseline configuration is indicated by flattening of the pressure distribution aft of 50% flap chord. This reversal of the flow away from the flap surface is responsible for inability of the main element wake to negotiate the adverse pressure gradient encountered over the upper

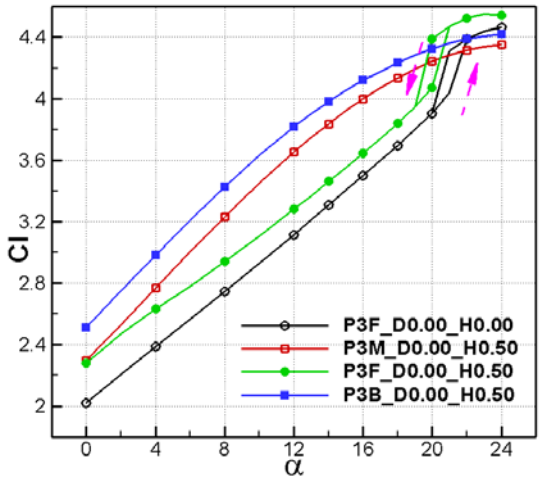

(a) Lift coefficient

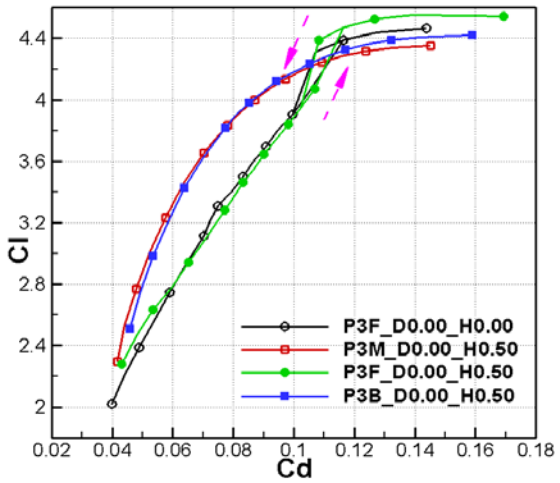

(b) Drag coefficient

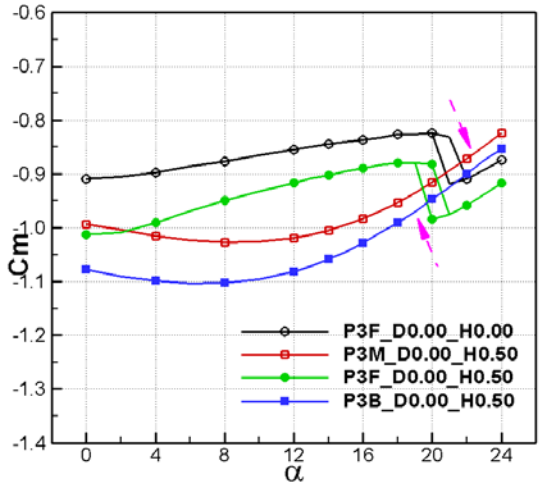

(c) Pitching moment coefficient

Fig.8 Effect of lift-enhancing tabs on the lift and moment coefficients of P3 baseline configuration

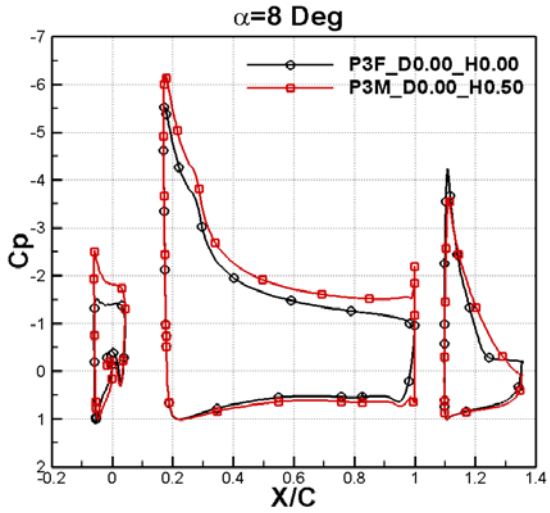

(a) Cove tab configuration

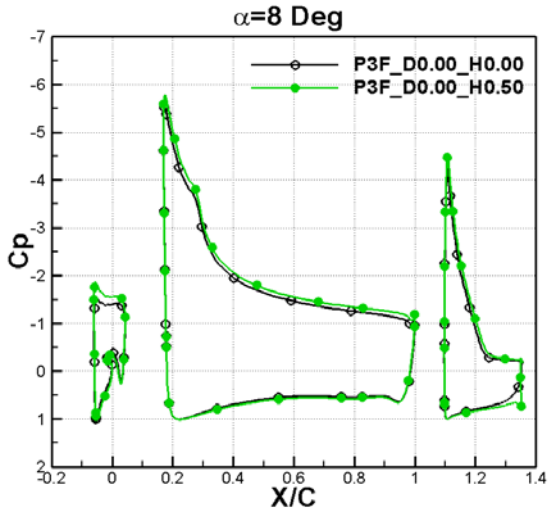

(b) Flap tab configuration

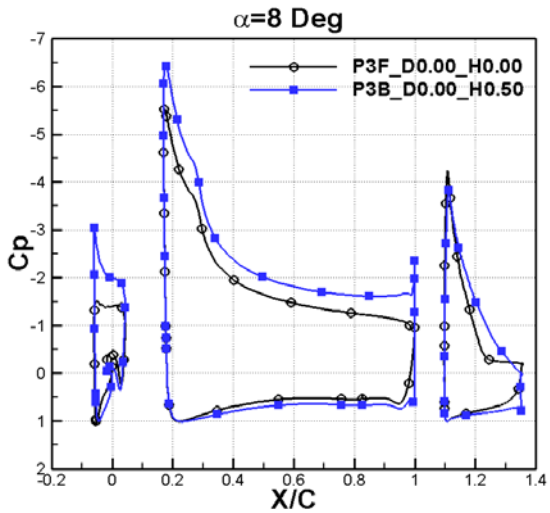

(c) Combination tab configuration

Fig.9 Effect of lift-enhancing tabs on the pressure distribution of a baseline configuration (α=8°)

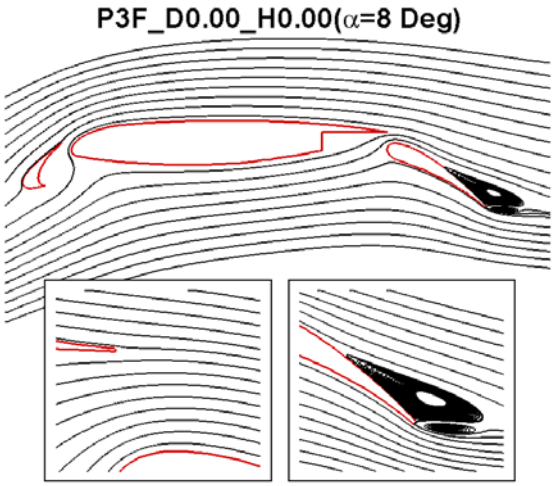

(a) Baseline configuration

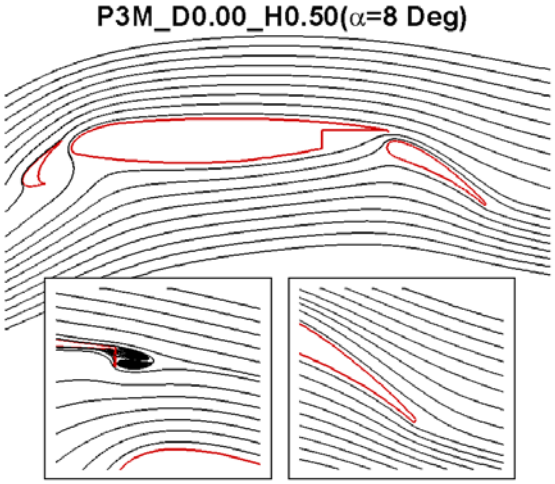

(b) Cove tab configuration

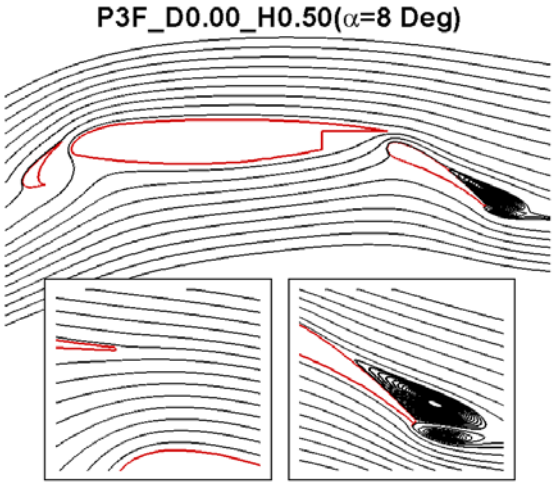

(c) Flap tab configuration

Fig.10 Streamline pattern around tab configurations (α=8°)

surface of the flap. The reduction in the flap suction peak attributed to the cove tab appears to eliminate a region of separated flow on the upper surface of the flap that exists for the baseline configuration. Separation elimination on the flap has a global effect on the flow over the entire high-lift system due to the "circulation effect" discussed by Smith [14] . Increased flap circulation leads to higher upper surface suction levels on the slat and main element. In addition, it's evident to observe the increased loading on the aft portion of the main element benefiting from increased aft camber due to the cove tab.

Computed streamlines at 8° angle of attack over baseline and cove tab configurations are illustrated in Fig.10(a) and (b) respectively. Separation on the baseline configuration is indicated by the large recirculation region over the aft 50% of the flap which leads to lift loss. However, adding of the cove tab induces attachment flow over the entire length of the flap. The flow field around the cove tab is dominated by a recirculating flow upstream and a two counter-rotating region downstream of the tab.

The cove tabs located at the main element trailing edge with height of 0.25%*c* and 0.75%*c* were also investigated, and the computed results indicated that increased tab height resulted in decreased slope of the lift curve and maximum lift coefficient. At an angle of attack of 8°, the corresponding lift coefficients were 3.16 and 3.24 respectively, and it was 3.23 for 0.50%*c* cove tab configuration mentioned previously.

When a 0.50%*c* flap tab was located on the baseline configuration, the hysteresis loop occurred earlier at angles of attack between 19° and 21°. The flap tab provides a lift increment that decreased more rapidly with angle of attack than the moderate flap gap case, which means that separation flow on the upper surface of flap affects the efficiency of flap tab. After all, lift coefficient increment at 8° angle of attack compared to the baseline configuration reaches 0.19, less than 0.26 at 0° angle of attack. The pressure distribution as shown in Fig.9(b) or streamline pattern of the flap tab configuration as shown in Fig.10(c) illustrates that the location of the separation point on the flap upper surface is nearly identical to that of the baseline configuration at 8° angle of attack. However, at 0° angle of attack the computed results not reported here showed that the separation point moved downstream slightly toward the trailing edge of flap. The change in drag coefficient can be negligible compared to the baseline configuration. The addition of a flap tab to the baseline configuration shifts the pitching moment coefficient curve in the negative direction.

As shown in Fig.8 and Fig.9, using the combination tab on the baseline configuration appears to be a linear combination of the above cove tab and flap tab. The combination tab provides the largest shift of lift coefficient as well as pitching moment coefficient, with drag coefficient at a constant lift coefficient almost identical to that for the cove tab configuration. An examination of the surface pressure distribution indicates that separation over flap of the baseline configuration is eliminated, which is mainly attributed to the tab located at the main element trailing edge.

3.3 Overall performance of lift-enhancing tabs

Effect of flap gap variations on lift coefficient are shown in Fig.11 for different configurations with and without lift-enhancing tabs. Note that the four configurations are differentiated with the flap gap and that of the two configurations not mentioned previously are 1.89%*c* and 2.39%*c* respectively, denoted as P1 and P2.

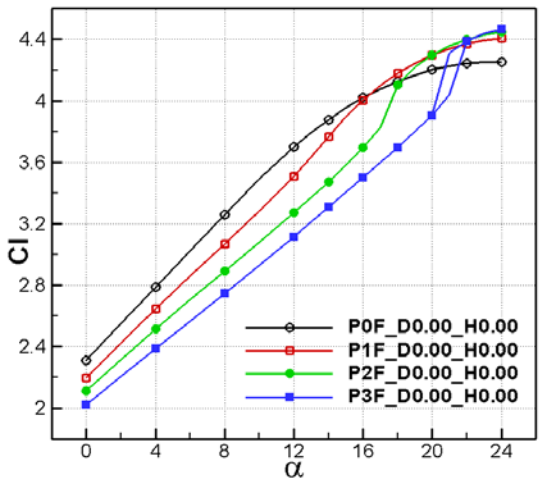

(a) Baseline configurations

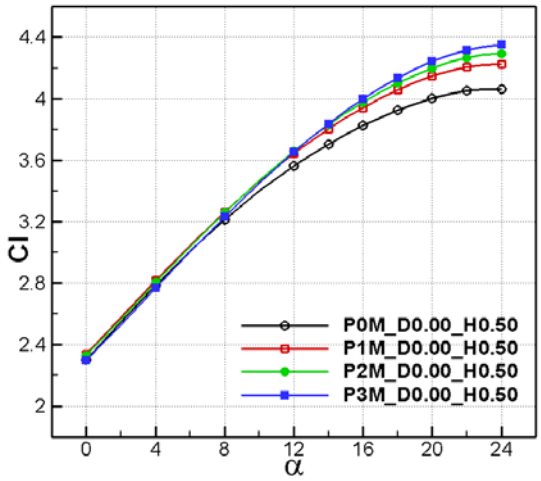

(b) Cove tab configurations

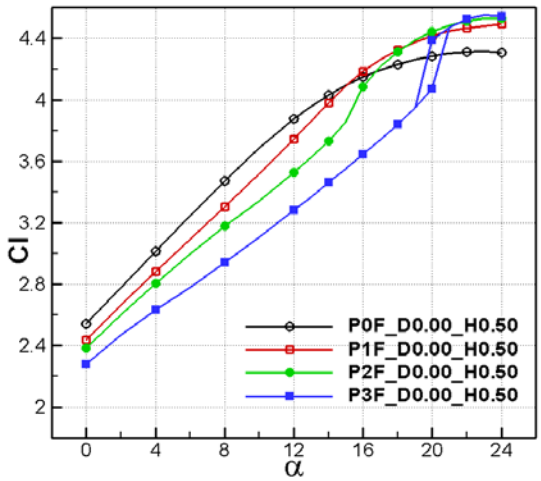

(c) Flap tab configurations

Fig.11 Effect of flap gap variations on tab configurations

The baseline performance of the Douglas three-element airfoil with a flap deflection angle of 30° is illustrated in Fig.11(a), showing strong sensitivity to the flap gap. As the flap gap was increased, the separation point moved upstream toward the flap leading edge rapidly, which leaded to a great loss in lift and a rapid rise in drag. The effect of an oversized flap gap is similar to increasing the Reynolds number with a fixed flap gap.

An interesting benefit from adding an appropriate cove tab to the baseline configuration is that they reduce the sensitivity to the flap gap, especially at low angles of attack, as shown in Fig.11(b). At present, the Reynolds number of wind tunnel experiments is far less than flight Reynolds number. Therefore in carrying high-lift system designs performed and optimized at a low Reynolds number to implementation on a production aircraft, Reynolds number effect can, in some instances, causes the performance to be less than expected. Fortunately, the cove tabs provide a simple means by which adjustments can be made to the effective gap, which means that the high-lift performance can be restored without redesigning and fabricating new flap tracks and actuators.

As shown in Fig.11(c), the use of flap tab on configurations with different flap settings can substantially increase the lift of the three-element airfoil, even in high flap gap case associated with potential separation over the upper surface of the flap. Therefore flap tabs would be useful as an inexpensive means of providing the increased high-lift performance sometimes necessary for growth versions of an aircraft without changing the existing high-lift system.

4 Conclusions

The effects of various lift-enhancing tabs on the Douglas three-element airfoil were numerically investigated for different flap riggings. The grids modeling the lift-enhancing tabs were blanked out from the computational domain of the baseline configuration and computed results showed its feasibility. In the moderate flap gap case, the cove tab adversely affects aerodynamic performance by reducing the suction peak on the flap. However, the appropriate cove tabs can effectively eliminate the separation on the upper surface of the flap with oversized gap, hence leading to an increase in lift and nose-down pitching moment as well as decreased drag. On a configuration with 2.89%c flap gap, the 0.50%c cove tab alone increased the lift coefficient at 8° angle of attack by 17.5%. In addition, cove tabs reduce the sensitivity of the lift of the multi-element airfoil to the size of the flap gap and may help to reoptimize an airfoil with the flap in non-optimum position. The flap tabs increase the lift and pitching moment coefficients with little drag penalty due to the increased aft camber of the flap, even in oversized flap gap cases, and these changes are

nonlinear with respect to the tab height. Adding a cove tab and a flap tab simultaneously to the baseline configuration appears to produce a linear combination of the changes caused by the individual tabs.

References

[1] Valarazo, W. O., Dominik C. J., McGhee, R. J., and Goodman, W. L. High Reynolds number configuration development of a high-lift airfoil. AGARD Conference Proceedings 515: High-lift Systems Aerodynamics-10, 1992.

[2] Klausmeyer, S. M., Papadakis, M. and Lin, J. C. A flow physics study of vortex generators on a multi-element airfoil. AIAA Paper 96-0548, 1996.

[3] Brunet, V., Garnier, E. and Pruvost, M. Experimental and numerical investigations of vortex generators effects. AIAA Paper 2006-3027, 2006.

[4] Singh, M. K., Dhanalakshmi, K. and Chakrabartty, S. K. Navier–stokes analysis of airfoils with gurney flap. *Journal of Aircraft*, Vol. 44, No. 5, 2007, pp. 1487-1493.

[5] Storms, B. L., Ross, J. C. An experimental study of lift-enhancing tabs on a two-element airfoil. AIAA Paper 94-1868, 1994.

[6] Ross, J. C., Storms B. L. and Carrannanto. Lift-enhancing tabs on multielement airfoils. *Journal of Aircraft*, Vol. 32, No. 3, 1995, pp. 649-655.

[7] Carrannanto, P. G., Storm, B. L., Ross J. C. and Cummins R. M. Navier-Stokes analysis of lift-enhancing tabs on multi-element airfoils. *Aircraft Design*, Vol. 1, No. 3, 1998, pp. 145-158.

[8] Rumsey, C. L., Ying, S. X. Prediction of high lift: review of present CFD capability. *Progress in Aerospace Sciences*, Vol. 38, 2002, pp. 145-180.

[9] Rogers, S. E. Progress in high-lift aerodynamic calculations. AIAA Paper 93-0194, 1993.

[10] Anderson, W. K., Bonhaus, D. L., McGhee, R. and Walker B. Navier-Stokes computations and experimental comparisons for multielement airfoil configurations. *Journal of Aircraft*, Vol. 32, No. 6, 1995, pp. 1246-1253.

[11] Chin, V. D., Peters D. W., Spaid F. W., and McGhee R. J. Flowfield measurements about a multi-element airfoil at high Reynolds numbers. AIAA Paper 93-3137, 1993.

[12] Biber, K. and Zumwalt, G. W. Hysteresis effects on wind tunnel measurements of a two-element airfoil. *Journal of Aircraft*, Vol. 31, No. 2, 1993, pp. 326-330.

[13] Yang, Z., Igarashi, H., Martin, M. and Hu, H. An experimental investigation on aerodynamic hysteresis of a low-Reynolds number airfoil. AIAA Paper 2008-0315, 2008.

[14] Smith, A. M. O. High-lift aerodynamics. *Journal of Aircraft*, Vol. 12, No. 6, 1975, pp. 501-530.

Copyright Statement